Published in final edited form as:

Neuron. 2018 January 03; 97(1): 221–230.e4. doi:10.1016/j.neuron.2017.11.020.

Old brains come uncoupled in sleep – Slow wave-spindle synchrony, brain atrophy and forgetting

Randolph F. Helfrich[1,2,5], **Bryce A. Mander**[3,4], **William J. Jagust**[1,4], **Robert T. Knight**[1,4,*], and **Matthew P. Walker**[1,4,*]

[1]Helen Wills Neuroscience Institute, UC Berkeley, 132 Barker Hall, Berkeley, CA 94720, USA

[2]Dept. of Psychology, University of Oslo, Forskningsveien 3A, 0373 Oslo, Norway

[3]Dept. of Psychiatry and Human Behavior, UC Irvine, 101 The City Dr, Orange, CA 92868, USA

[4]Dept. of Psychology, UC Berkeley, Tolman Hall, Berkeley, CA 94720, USA

Summary

The coupled interaction between slow wave oscillations and sleep spindles during non-rapid-eye-movement (NREM) sleep has been proposed to support memory consolidation. However, little evidence in humans supports this theory. Moreover, whether such dynamic coupling is impaired as a consequence of brain aging in later life, contributing to cognitive and memory decline, is unknown. Combining, electroencephalography (EEG), structural MRI and sleep-dependent memory assessment, we addressed these questions in cognitively normal young and older adults. Directional cross-frequency coupling analyses demonstrated that the slow wave governs a precise temporal coordination of sleep spindles, the quality of which predicts overnight memory retention. Moreover, selective atrophy within the medial frontal cortex in older adults predicted a temporal dispersion of this slow wave-spindle coupling, impairing overnight memory consolidation leading to forgetting. Prefrontal dependent deficits in the spatiotemporal coordination of NREM sleep oscillations provide a potential pathway to age-related memory decline.

eTOC blurb

Helfrich et al. demonstrate that the precise coupling between sleeping brainwaves, called slow waves and spindles, supports memory retention. However, this brainwave coupling during sleep is impaired in older adults due to loss of tissue in the medial frontal lobe, resulting next-day forgetting.

Corresponding author: Randolph F. Helfrich, 132 Barker Hall, Knight Lab, Helen Wills Neuroscience Institute, University of California, Berkeley, CA 94720-3190, USA, phone: +1-510-6430-9744. rhelfrich@berkeley.edu.
[5]Lead Contact
[*]These authors contributed equally

Author Contributions

Conceptualization, R.F.H., B.A.M., W.J.J., R.T.K., M.P.W.; Methodology, R.F.H.; Software, R.F.H., B.A.M.; Validation, R.F.H., B.A.M.; Formal Analysis, R.F.H., B.A.M.; Investigation, B.A.M.; Resources, W.J.J., R.T.K., M.P.W.; Data Curation, R.F.H., B.A.M., M.P.W.; Writing – Original Draft, R.F.H.; Writing – Review & Editing, R.F.H., B.A.M., R.T.K., M.P.W.; Visualization, R.F.H.; Supervision, R.T.K., M.P.W.; Project Administration, B.A.M., M.P.W.; Funding Acquisition, W.J.J., R.T.K., M.P.W.

Introduction

The precise temporal coordination of NREM sleep oscillations has been proposed to support the long-term consolidation of memory (Diekelmann and Born, 2010; Walker and Stickgold, 2006). Within these theoretical frameworks, temporal interactions between cortical slow oscillations (SO; < 1.25 Hz), sleep spindles (~12–16 Hz), and hippocampal ripples (~80–100 Hz) form a hierarchy that allows for information transformation necessary for long-term memory retention (Diekelmann and Born, 2010; Frankland and Bontempi, 2005; Latchoumane et al., 2017; Rasch and Born, 2013; Staresina et al., 2015). In particular, the depolarizing 'up-states' of the SO are proposed to facilitate sleep spindle and ripple expression, with hippocampal ripples being temporally nested into spindle troughs (Rasch and Born, 2013; Staresina et al., 2015). The coupling of these NREM oscillations is thought to support intrinsically timed information transfer across several spatiotemporal scales underlying long-term memory (Diekelmann and Born, 2010).

There is, however, limited empirical evidence supporting this oscillatory interaction model of hippocampal memory consolidation. Non-invasive brain stimulation findings have demonstrated that boosting SO power can indirectly co-modulate sleep spindle activity (Ladenbauer et al., 2017; Marshall et al., 2006), while SO-spindle coupling during a nap in young adults tracks offline memory retention (Niknazar et al., 2015). Yet the mechanistic relationship of SO-spindle synchrony, and how this determines the success or failure of overnight hippocampal-dependent memory consolidation remains unknown, as does the causal necessity of brain regions in supporting coupled NREM oscillation dynamics and memory benefit.

Regarding the latter, there is growing evidence that aging markedly disrupts sleep and overnight memory consolidation (Mander et al., 2017). If sleep oscillatory coupling is compromised in older adults, what it is about the aging brain that degrades interactive synchrony of NREM oscillations leading to memory impairment? This question is of special relevance as it may reveal a currently under-appreciated mechanism (impaired SO-spindle coupling) that contributes to memory decline in later life, and if identified, would defined a novel therapeutic target for clinical intervention (Ladenbauer et al., 2017).

Here, we address these unanswered questions by combining structural MRI, polysomnography with full-head (19 channel) scalp electroencephalography (EEG), and the assessment of sleep-dependent hippocampal memory, in young and older adults. We specifically tested the hypothesis that the precise temporal coupling of cortical NREM SO-spindles, as predicted by theoretical models, facilitates overnight memory retention in young adults, and whether older adults have a temporal un-coupling of these oscillations leading to impaired overnight memory. Moreover, based on evidence in young and older adults demonstrating that the structural grey-matter morphology of the medial prefrontal cortex (mPFC) is associated with the quality of SO (Mander et al., 2013; Saletin et al., 2013), and that this same mPFC region is an EEG source generator of SO linked to spindles (Murphy et al., 2009), we further tested the hypothesis that structural grey matter integrity of mPFC predicts the degree of compromised SO-spindle dynamic coupling in older adults.

We implemented unique non-linear directional cross-frequency coupling (CFC) analyses, together with phase-dependent correlation measures, to capture complex neural dynamics underlying SO-spindle synchrony relationships (Helfrich and Knight, 2016). Based on theoretical accounts of oscillation-based timed memory transfer (Diekelmann and Born, 2010; Rasch and Born, 2013), we tested the hypothesis that the exact timing between SO and spindles supports memory consolidation. Building on the prediction that SO orchestrate sleep-dependent memory networks (Steriade, 2006), we implemented methods for assessing the temporal directionality of this SO-spindle interaction (Jiang et al., 2015), and examined if this directionality predicted memory consolidation success in young and older adults. Finally, we tested whether regional gray matter atrophy within the mPFC, relative to other control regions, provided a structural correlate associated with the age-related degradation of SO-spindle coupling and associated memory decline in older adults.

Results

Cognitively normal older (n = 32; age: 73.8 ± 5.3; mean ± SD) and young (n = 20; 20.4 ± 2.0 years) participants performed a sleep-dependent episodic memory test (Mander et al., 2013, 2015) before and after a full night of sleep (Figure 1A and Table S1–S3). After encoding, all participants were trained to 100% criterion before initial recognition testing (short delay; after ~10 min). After the short delay test, participants underwent polysomnography in the lab and were given an 8 h sleep period starting at their habitual bedtime. They performed the second recognition test (long delay; after ~10 h) the next morning. Then structural MRI data to assess gray matter (GM) intensity were obtained. Memory retention was quantified as the difference between recognition performance at the long delay minus performance at the short delay. Consistent with existing reports (Mander et al., 2013, 2017), overnight memory retention was impaired in older adults relative to young adults ($t_{46} = -3.85$, $p = 0.0004$, $d = 1.19$), leading to the next-step quantification of differences in NREM oscillatory dynamics that may underlie these age-associated memory impairments.

Oscillatory dynamics of sleep in old and young adults

We first assessed EEG power differences between older and young adults by means of cluster-based permutation tests across all frequencies and channels during NREM sleep (Figure 1B; with all figures displaying data from electrode Cz due to the spatial distribution of SO and spindle power, unless stated otherwise). Oscillatory power was significantly lower in older adults from 0.5 to 8.5 Hz ($p = 0.0020$, $d = 1.71$) as well as between 10.5 and 15 Hz ($p = 0.0080$, $d = 1.28$) in all recorded channels (Figure 1B).

Next, we detected SO (0.16 – 1.25 Hz) and sleep spindle (12 – 16 Hz) events based on established algorithms (Mölle et al., 2011; Staresina et al., 2015). Analysis of inter-spindle intervals indicated that sleep spindles exhibited a non-Poisson like behavior and were preferentially separated by 1.13 – 2.78 s during NREM sleep (Figure S1A), which is in accordance with the idea that < 1 Hz SO controls sleep spindle timing and separates them by at least 1–3 cycles.

Detection of SO and sleep spindle events reliably tracked spectral sleep signatures over a full night of sleep (Figure 1C/D for exemplary old/young subjects; numbers of detected events are superimposed in white; see also Table S2). For every participant, we determined the SO phase during the peak of the detected sleep spindle events. Significant non-uniform circular distributions were identified in 29/32 old adults and in 20/20 young adults. Of note, differences in oscillatory power can distort cross-frequency coupling estimates. This issue was addressed by z-normalizing individual events in the time domain to alleviate amplitude differences prior to all subsequent analyses (Figure 2A and Table S4). Note that this normalization avoids spurious coupling that has been recently pointed out as a potential confound in cross frequency analysis (Aru et al., 2015; Cole and Voytek, 2017; Gerber et al., 2016). To further address this concern, we also employed a validated stratification approach (Aru et al., 2015), confirming our main findings (Figure S1B/C).

Aging affects prefrontal SO-spindle coupling

Following normalization, SO trough-locked time-frequency spectrograms were first calculated separately for older and young adults and then compared using a cluster-based permutation approach. Multiple significant clusters were observed in the sleep spindle range (Figure 2B; $p = 0.0160$, $d = 1.73$). Interleaved patterning in the spindle range (white dashed box, Figure 2B) demonstrated that the timing of sleep spindles relative to the SO was different between older and young adults. Specifically, spectrograms illustrated that sleep spindles peaked before, rather than in time with, the SO peak in older relative to young adults (Figure S2A and inset in Figure 2C).

Mean sleep spindle activity was nested just after the SO peak in young adults, but was misaligned in older adults, occurring earlier in the rising flank of the SO (see Figure 2B/C). Significant non-uniform distributions were present for both older (Rayleigh $z = 23.24$, $p < 0.0001$) and young adults (Rayleigh $z = 18.55$, $p < 0.0001$). However, the mean coupling direction differed significantly between groups (Figure 2D; older adults: −46.3° ± 31.2°; young adults: 3.6° ± 15.5°; circular mean ± SD; Watson-Williams test: $F_{1,50} = 41.34$; $p < 0.0001$; $\eta^2 = 0.44$). That is, spindles in young adults were maximal just after the SO peak, while sleep spindles in older adults were misaligned, prematurely peaking earlier on the rising phase in the SO cycle. This effect was not confounded by differences in spindle onset phase angles or differences in spindle duration (Figure S1D–F).

Next, we assessed differences in coupling strength between groups using two complimentary analyses: 1) an event-locked coupling approach that extracted the resultant vector length per subject for all SO-spindle events at every electrode, and 2) a data-driven approach based on the modulation index and screening of a wide-range of phase-amplitude pairs.

For the first analysis, significant cluster difference in frontal topography was identified older and young adults ($p = 0.0120$, $d = 0.76$), indicating that SO-spindle coupling was most impaired over fronto-central sensors (Figure 2E). The second, data-driven analysis, confirmed that this fronto-central cluster effect was specific to the SO-range between the 0.5 – 2 Hz and the 12 – 16 Hz range ($p = 0.0150$, $d = 0.92$), indicating that stronger coupling in young adults was limited to the SO-spindle range (Figure 2F and Figure S2B). Both

approaches were highly correlated (rho = 0.7645, $p < 0.0001$) and effects were not simply driven by differences in the number of oscillatory events (Figure S1G/H).

Cortical slow oscillations coordinate spindle activity

Having established differences in SO-spindle coupling between young and older adults, and building on our hypothesis and past theoretical models of SO driving spindle coordination, we next investigated directional influences between SO and sleep spindles by means of the phase slope index (PSI).

A cluster-based permutation test revealed that the directional influence of SO on sleep spindle activity was impaired in older as compared to young adults over frontal and parieto-occipital regions (Figure 2G; $p = 0.0010$, $d = 0.81$). However, while parieto-occipital directional CFC was markedly reduced in older adults, it was still above zero (Figure S2C). This demonstrates that the parietal physiologic SO-spindle coupling was partially intact in older adults.

To examine directionality, we tested whether the PSI predicted how much time the sleep spindle deviated from the SO peak. A significant frontal cluster was identified over fronto-central sensors, indicating that larger PSI values predicted a smaller deviance — that is, a sleep spindle peak closer to the ‘upstate’ in young relative to older adults ($p = 0.012$, mean rho = −0.3367; older adults: 205.07 ± 18.68 ms; young adults: 60.24 ± 8.26 ms; mean ± SD). This PSI analysis demonstrated two findings: 1) The SO phase predicts spindle timing over frontal sensors, rather than the converse, as postulated by theoretical models that SO triggers spindle events, and 2) the timing precision was misaligned, since directional influences were reduced in older relative to young adults.

SO-spindle coupling predicts overnight memory consolidation

Having characterized the oscillatory dynamics of SO-spindle coupling and identified impairments in these dynamics in older relative to young adults, we tested our hypothesis that these oscillatory dynamics predicted overnight memory retention success, and associated age-related differences. Note that traditional linear correlation analyses were not applicable given that phase is a circular metric. Cluster-corrected circular-linear correlation analyses (see Methods) were used to assess the non-linear relationship between optimal coupling phase and behavior.

A significant positive cluster was identified over frontal regions ($p = 0.0010$, mean rho = 0.4353) peaking at electrode F3 (rho = 0.5699; Figure 3A). To further delineate and visualize this non-linear relationship, we binned the average memory retention scores relative to the individual mean coupling direction (10 bins, overlap: ±1 bin; grey shaded; Figure 3A). The resulting distribution followed an inverted u-shape, demonstrating that the success of overnight memory consolidation was achieved when the spindle event occurred most proximal to the SO ‘up-state’ peak. When spindles occurred further from that ‘up-state’ peak, the predictive influence on overnight memory retention success declined. Note this finding was not confounded by demographic or sleep architecture differences (Table S5).

No other significant EEG clusters were identified when SO-spindle coupling strength was correlated with the degree of overnight memory retention across all subjects (Figure 3B). To assure that these results were robust against differences in oscillation power and peak frequency (Table S4), we corrected for sleep spindle peak and amplitude distribution confounds (Figure 3C and Figure S3) by detecting the individual sleep spindle peak frequency for every SO event. A significant positive cluster was observed ($p = 0.0040$, mean rho = 0.3790), which peaked at electrode C4 (Figure 3D, rho = 0.4705) indicating that the coupling phase robustly predicted overnight memory retention.

Importantly, this effect peaked in both older and young adults at neighboring electrodes (C4 in older adults: rho = 0.5725; Cz in young adults: rho = 0.5678). This result demonstrates that, even though older adults showed a reduction in SO-spindle coupling, and lower overnight memory retention than young adults, the same predictive functional relationship between SO-spindle coupling and memory consolidation success was observed in both groups.

Performance for older and young adults was binned, allowing the expression of the quadratic fits to highlight the inverse u-shaped relationship indicated by the circular-linear correlations (Figure 3D). These findings confirmed that after correcting for power and peak frequency differences, the degree of overnight memory retention success was still predicted by the timing of the coupled relationship between the SO and spindle (Figure 3D). Therefore, memory consolidation success was most accurately predicted by sleep spindle amplitude peaking just after the SO ‘up-state’ peak.

Age-related grey matter atrophy predicts coupling deficits

Collectively, the above analyses established 1) the oscillatory dynamics of SO-spindle coupling, demonstrated impairments in these dynamics in older relative to young adults, and 2) identified that the spatiotemporal precision of SO-spindle coupling predicted the degree of overnight memory retention success and when impaired in older adults, predicted greater overnight forgetting.

Finally, we sought to determine a potential underlying pathological mechanism accounting for why older adults suffer these impairments. We focused *a priori* on mPFC grey matter, based on the prominent role of the mPFC in SO oscillatory generation (Murphy et al., 2009; Saletin et al., 2013). Specifically, we tested the hypothesis that mPFC grey matter atrophy predicts the degree of compromised SO-spindle dynamic coupling.

To rule out age-related confounds, we corrected all structural metrics by the total intracranial volume, which were correlated (rho = −0.2919, $p = 0.0358$). We then utilized cluster-based permutation correlation analyses to assess whether the grey matter volume in any ROI predicted directional SO-spindle coupling as measured by the PSI. Consistent with the hypothesis, grey matter volume in mPFC positively correlated with directional coupling (Figure 4A; $p = 0.0080$, mean rho = 0.3321), indicating that as grey matter volume in mPFC decreases, directional phase coupling between SO and sleep spindles is weakened. Note, that the results were comparable when we corrected for total brain volume (rho = 0.29, p =

0.0343). In addition, we partialled out age from the cluster-based correlation test (see Methods) and again obtained a significant frontal cluster (p = 0.0490; mean rho = 0.25).

While our results confirmed the key role of SO in the coupling dynamics and associated memory consolidation benefit, sleep spindles, which are grouped by the SO, are anatomically recognized to be thalamo-cortical mediated events (Steriade et al., 1987; though spindles have also been measured in the hippocampus; De Gennaro and Ferrara, 2003; Staresina et al., 2015). Given these findings we performed additional post-hoc analyses to examine whether grey matter volume in these spindle-associated regions also predicted impairments in SO-spindle coupling the associated memory benefit.

Grey matter volume was extracted for all regions of interest (ROI) where sleep related oscillations are thought to emerge: hippocampus and the thalamus, in addition to the neighboring lateral orbitofrontal cortex (OFC) or dorsolateral PFC (DLPFC) and several control ROIs (occipital, precuneus, posterior cingulate cortex and posterior parietal cortex), but no significant effects were observed for these other eight ROIs (Figure 4B). These results confirmed the key role of mPFC in altered SO-spindle coupling – an anatomical-physiological relationship that was not observed for other likely candidate regions.

Discussion

Together, our results provide the first demonstration that 1) the precisely coordinated timing between the cortical NREM SO ‘up-state’ and the sleep spindle predicts successful hippocampus-dependent memory consolidation. 2) Temporal disruption of this coordinated NREM oscillation coupling in older relative to young adults predicts impaired hippocampus-dependent overnight memory consolidation. 3) One pathological mechanism associated with impairment in spatiotemporal coupling of the cortical SO with sleep spindles in older adults is the severity of mPFC gray matter atrophy.

The oscillatory hierarchy of sleep-dependent memory consolidation

A long-standing proposal in models of sleep-dependent hippocampus-dependent memory consolidation involves the timed interactive coupling between SO and sleep spindles (Rasch and Born, 2013). Indirect evidence to date has involved demonstrating that individual properties of SO and sleep spindles are linked to successful overnight memory retention (Niknazar et al., 2015; Mander et al., 2013; Gais et al., 2002; Mander et al., 2014; Mölle et al., 2002). Seminal intracranial EEG studies have further highlighted the hierarchical coupling of cortical SO, cortico-thalamic sleep spindles, and hippocampal ripples (Clemens et al., 2007; Mak-McCully et al., 2017; Staresina et al., 2015). However, no assessment of memory was performed in these studies, leaving the functional relevance of these coupled NREM oscillation relationships unclear. Moreover, no direct assessment of the directionality of the coupling of these events has been reported.

Here, we address these issues using directional cross-frequency coupling analyses (Helfrich and Knight, 2016), and determined how SO modulate sleep spindle timing, amplitude, and peak frequency. Our results reveal a unique spatiotemporal profile of the coupling relationship between SO and sleep spindles in young adults, such that sleep spindle

amplitude peaked around the cortical ‘up-state’. Moreover, this precise temporal relationship was especially pronounced over centro-parietal regions—of topographical relevance as it may be considered the anatomical convergence zone between the known frontal dominance of the SO (Murphy et al., 2009) and the parietal dominance of broad-range (11–16 Hz) spindles (De Gennaro and Ferrara, 2003; Riedner et al., 2011).

A second key finding revealed by the current study is that the normally precise spatiotemporal coordination of the SO-spindle coupled event is impaired in older adults. Unlike young adults, in which spindle events expressed a strong coincidence with the cortical SO ‘up-state’, spindle oscillations in older adults arrived, on average, further away from the depolarizing upswing of the SO cycle, occurring prior to it rather than just after the depolarization envelop. In addition, this phase coupling was more dispersed over SO in older adults. These findings provide evidence that the aging brain loses the neurophysiological ability to coordinate the two dominant oscillations of NREM sleep, in stark contrast to the precise spatiotemporal coupling expressed in young adults. However, these data alone do not necessarily establish that this dynamic coupling profile is of functional benefit in young adults, and whether coupling impairments in older adults is detrimental for older adults. We address this issue next.

SO-spindle coupling and overnight memory consolidation

System consolidation theory suggests that new memories are transiently more dependent on the hippocampus and then gradually transform to become more prefrontal-dependent (Frankland and Bontempi, 2005; Kitamura et al., 2017). Endogenous NREM oscillatory activity is thought to provide the key functional substrate of timed information transfer between cortical regions (Buzsáki and Draguhn, 2004). In particular, neocortical SO are thought to orchestrate thalamo-cortical sleep spindle and hippocampal ripple activity during NREM sleep to facilitate the information transfer between neocortical and hippocampal circuits (Buzsáki, 1998; Isomura et al., 2006; Sirota et al., 2003). This nesting of multiple frequency bands constitutes an oscillatory hierarchy, providing the precise intrinsically-generated timing to route information from the hippocampus to neocortical areas at times of high excitability, which in turn facilitate long-term storage (Born and Wilhelm, 2012; Diekelmann and Born, 2010).

Several studies have inferred a role of the phase of the SO in determining the success of memory consolidation using indirect measures (Batterink et al., 2016; Papalambros et al., 2017). In addition, brain stimulation studies have established that entrainment of SO can have reciprocal effects on sleep spindles, and vice versa (Lustenberger et al., 2016; Marshall et al., 2006). Most recently, it has been suggested that shifts in the exact SO-spindle timing could give rise to the behavioral benefits of electrical stimulation observed in rodents, which may also be beneficial in cognitively impaired older individuals (Ladenbauer et al., 2017; Latchoumane et al., 2017; Niknazar et al., 2015). Our results provide the first direct evidence that the exact timing of SO and sleep spindles in the healthy, human brain predicts the success of overnight hippocampus-dependent memory retention (Diekelmann and Born, 2010; Mander et al., 2017).

A further discovery of the current study is the demonstration that the precise temporal interplay of SO and sleep spindles is disrupted in older adults, wherein sleep spindles were misaligned (often occurring too early in the SO cycle) relative to the precise timing in young adults. The process of human brain aging appears to weaken the otherwise robust NREM oscillatory hierarchy, reducing the optimal SO-spindle phase timing, and in doing so, predicts impaired memory consolidation. Two points are of relevance in this regard. First, the finding that the memory-SO-spindle coupling relationship was significant in older adults, but at an earlier phase, demonstrates that both SO and sleep spindles were still expressed in older adults. However, the mechanism that couples them in time is impaired, with spindles systematically arriving too early within the SO cycle. Second, it establishes that this impaired SO-spindle temporal coupling diminished the magnitude of overnight memory consolidation benefit.

Neurophysiological correlates of age-related memory decline

A multitude of studies demonstrated that aging affects sleep architecture and memory (Mander et al., 2017). However, no neurophysiological mechanism has been identified that functionally links age-related changes in sleep physiology to impaired memory retention, beyond quantitative reductions in the amount of oscillatory activity. Here, we provide evidence that addresses this mechanistic gap in understanding, demonstrating the loss of temporal SO-spindle coupling over specific topographical regions explains the degree of failed of memory consolidation.

Interestingly, when only focusing on the basic phase measure, sleep spindles lock as precisely to the rising flank of the SO in older adults as they do young adults, as we show in Figure 2C/D. However, our directional phase analyses revealed the existence of a clear age-related deficit. Specifically, inspection of SO-spindle interactions, shown in Figure 2G, demonstrated that the directional influence of SO on sleep spindle timing was diminished in older adults relative to young adults, resulting in a misaligned arrival of the spindle relative to the SO. Moreover, we found that this age-related impairment was not equivalent across all brain regions, but was expressed most significantly over prefrontal cortex sensors and less strongly over parieto-occipital regions (Figure 2G and Figure S2C). These results further establish that, in later adult life, the human adult brain experiences a decline in the ability to precisely coordinate SO with cortico-thalamic sleep spindles. Specifically, spindles occur more often at unfavorable SO phases in older adults, arriving too early to confer optimal hippocampus-dependent memory consolidation benefits.

One testable hypothesis in animal models emerging from our findings is that the impaired coordination of temporal SO-spindle coupling over prefrontal cortex does not trigger hippocampal ripples as effectively, and that the magnitude of that failure should predict the consequential degree of impaired rather than successful sleep-dependent memory consolidation (Rosanova and Ulrich, 2005).

Prefrontal atrophy, SO-spindle coupling and aging

Beyond impairments in memory-relevant SO-spindle coupling in older relative to young adults, we further established at least one pathological alteration contributing to the severity

of this age-related coupling dysfunction— grey matter atrophy within the mPFC. Grey matter volume of the medial prefrontal cortex predicts inter-individual differences in the quality of SO in both young (Saletin et al., 2013) and older (Mander et al., 2013) adults. Moreover, high-density EEG evidence has defined a role for the mPFC in the generation of slow waves (Murphy et al., 2009).

Our findings advance this anatomical-neurophysiological connection. We show that the decrease in structural integrity of the mPFC accounts for the qualitative degree of impaired temporal phase coupling between the SO and sleep spindles. Thus, mPFC atrophy, in addition to reducing SO incidence and intensity (Mander et al., 2013; Saletin et al., 2013), contributes to misalignment of the timing of sleep spindles relative to the SO phase. This effect is greatest over frontal EEG derivations, indicating that the mPFC may play a particularly important role in the regulation of the coordinated timing of NREM sleep oscillations.

The results reveal that the structural integrity of mPFC is one factor determining the capacity of the human brain to precisely and optimally coordinate the timed arrival of sleep spindles with the SO, and in doing so, dictate the success or failure of hippocampus-dependent memory consolidation. Intracranial studies taking advantage of invasive recordings from multiple regions of interest in concert, such as mPFC, the hippocampus, and thalamus (Clemens et al., 2007; Mak-McCully et al., 2017; Nir et al., 2011; Staresina et al., 2015) will help to clarify the directional influences of cortical-subcortical interaction not possible with scalp EEG recordings. Such recordings occurring combined with sleep-dependent memory tasks would further our current understanding of the coordinated interactions between the mPFC, thalamus, and hippocampus that occurs during NREM sleep oscillations, as well as their necessity and sufficiency in supporting long-term memory retention.

Conclusions

Our findings reveal a fundamental neurophysiologic mechanism involving the spatiotemporal coupling between the SO and the sleep spindle, and demonstrate that this temporal synchrony is functionally and behaviorally relevant for the success of overnight memory consolidation. We further show that this same neurophysiological oscillatory dynamic is impaired in older relative to young adults, leading to imprecise sleep spindle expression in relationship with the depolarizing ‘up-state’ of the SO. Moreover, our findings reveal that age-related prefrontal gray matter atrophy represents one neuropathological substrate explaining the attenuation of this oscillatory control mechanism, which thus impairs hippocampus-dependent memory consolidation.

Our results are of potential clinical relevance in two ways. First, they document the presence of an under-appreciated pathway—impaired temporal precision of sleep oscillation coupling —that contributes to memory decline in later life. Second, they help define sleep oscillatory synchrony as a novel therapeutic target for modulation of hippocampus-dependent memory consolidation in older adults, and potentially in those with mild cognitive impairment (Ladenbauer et al., 2017) and Alzheimer’s disease (Mander et al., 2017). This may be achieved using non-invasive entrainment by means of acoustic, electric, or magnetic brain

stimulation (Helfrich et al., 2014; Papalambros et al., 2017), aiming to restore the temporally precise SO-spindle coordination (Marshall et al., 2006) closer to that of young adults, helping reduced the impact of cognitive decline in aging.

STAR METHODS

CONTACT FOR REAGENT AND RESOURCE SHARING

Further information and requests for resources and reagents should be directed to and will be fulfilled by the lead contact, Randolph Helfrich (rhelfrich@berkeley.edu).

EXPERIMENTAL MODEL AND SUBJECT DETAILS

Participants—32 healthy older (mean age: 73.7 ± 5.3; mean ± SD) and 20 younger adults (20.4 ± 2.0 years) participated in the study (see Table S1 for demographic details). All participants provided written informed consent according to the local ethics committee (Berkeley Committee for Protection of Human Subjects Protocol Number 2010-01-595) and the Declaration of Helsinki. Data from a subset of participants has been reported previously (Mander et al., 2013, 2014, 2015).

METHOD DETAILS

Experimental design and procedure—All participants were trained on the episodic word-pair task in the evening and performed a short recognition test after 10 min. Then, participants were offered an 8 h sleep opportunity, starting at their habitual bedtime. Polysomnography was collected continuously. Participants performed a long version of the recognition test approximately 2 h after awakening. Subsequently, we obtained structural MRI scans from all participants. Two older adults did not complete behavioral testing, and two young adults failed to achieve criterion at encoding. Thus, these four subjects were excluded from behavioral analyses, but were included in all electrophysiological and imaging analyses.

Behavioral task—We utilized a previously established sleep-dependent episodic memory task (Figure 1A), where subjects had to learn word-nonsense word pairs (Mander et al., 2013). In brief, words were 3–8 letters in length and drawn from a normative set of English words, while nonsense words were 6–14 letters in length and derived from groups of common phonemes. During encoding, subjects learned 120 word-nonsense pairs. Each pair was presented for 5 s. Participants performed the criterion training immediately after encoding. The word was presented along with the previously learned nonsense word and two new nonsense words. Subjects had to choose the correctly associated nonsense words and received feedback afterwards. Incorrect trials were repeated after a variable interval, and were presented with two additional new nonsense words to avoid repetition of incorrect nonsense words. Criterion training continued until correct responses were observed for all trials.

During recognition, a probe word or a new (foil) probe word was presented along with 4 options: (1) the originally paired nonsense word, (2) a previously displayed nonsense word, which was linked to a different probe (lure), (3) a new nonsense word or (4) an option to

indicate that the probe is new. During the recognition test after a short delay (10 min), 30 probe and 15 foil trials were presented. At the long delay (10 h), 90 probe and 45 foil trials were tested. All probe words were presented only once during recognition testing, either during short or long delay testing.

Sleep monitoring and EEG data acquisition—Polysomnography (PSG) sleep monitoring was recorded on a Grass Technologies Comet XL system (Astro-Med), including 19-channel electroencephalography (EEG) placed using the standard 10–20 system as well as Electromyography (EMG). Electrooculogram (EOG) was recorded the right and left outer canthi. EEG recordings were referenced to bilateral linked mastoids and digitized at 400 Hz in the range from 0.1 – 100 Hz. Sleep scoring was performed according to standard criteria in 30 s epochs (Rechtschaffen and Kales, 1968) (See Table S2 for sleep stage metrics for each group). Slow wave sleep (SWS) was defined as NREM stages 3–4, while NREM sleep encompassed stages 2–4. Given that stage 2 does not always exhibit pronounced SO activity (Figure 1C/D), we focused on SWS for all correlational analyses.

MRI data acquisition—Scanning was performed on a Siemens Trio 3T scanner with a 32-channel head coil. We obtained two high-resolution T1-weighted anatomical images, which were acquired using a three-dimensional MPRAGE protocol with the following parameters: repetition time, 1900 ms; echo time, 2.52 ms; flip angle, 9°; field of view, 256 mm; matrix, 256 × 256; slice thickness, 1.0 mm; 176 slices. MPRAGE images were co-registered, and the mean image was used to perform optimized voxel-based morphometry (VBM) to examine grey matter volume within specified regions of interest (ROI) as described below.

QUANTIFICATION AND STATISTICAL ANALYSIS

Behavioral data analysis—Memory recognition was calculated by subtracting both the false alarm rate (proportion of foil words, which subjects' reported as previously encountered) and the lure rate (proportion of words that were paired with a familiar, but incorrect nonsense word) from the hit rate (correctly paired word-nonsense word pairs). Memory retention was subsequently calculated as the difference between recognition at long minus short delays.

EEG data

Preprocessing: EEG data were imported into EEGLAB and epoched into 5 s bins, which were visually inspected for artifacts. Then the continuous data was exported to FieldTrip for further analyses.

Spectral analysis: (1) To obtain the average power spectra (Figure 1B), the raw data was epoched into non-overlapping 15 second segments and epochs containing artifacts were rejected. Data was tapered with a Hanning window and spectral estimates were calculated from 0.5 to 50 Hz in 0.5 Hz steps and averaged per subject and channel for all epochs in NREM sleep. (2) To obtain a continuous time-frequency representation of a whole night of sleep (Figure 1C/D), we utilized multitaper spectral analyses (Mitra and Pesaran, 1999; Prerau et al., 2017), based on discrete prolate slepian sequences. The raw data was epoched into 30 second long segments, with 85% overlap. Spectral estimates were obtained between

0.5 and 30 Hz in 0.5 Hz steps. We utilized 29 tapers, providing a frequency smoothing of ± 0.5 Hz.

Event detection: Event detection (Figure 1D and Figure 2A/C) was performed for every channel separately based on previously established algorithms (Mölle et al., 2011; Staresina et al., 2015). (1) Slow oscillations: In brief, we first filtered the continuous signal between 0.16 and 1.25 Hz and detected all the zero crossings. Then events were selected based on time (0.8 – 2 s duration) and amplitude (75% percentile) criteria. Finally, we extracted artifact-free 5 s long segments (± 2.5 s around trough) from the raw signal. (2) Sleep spindles: We filtered the signal between 12–16 Hz and extracted the analytical amplitude after applying a Hilbert transform. We smoothed the amplitude with a 200 ms moving average. Then the amplitude was thresholded at the 75% percentile (amplitude criterion) and only events that exceeded the threshold for 0.5 to 3 s (time criterion) were accepted. Artifact-free events were then defined as 5 s long sleep-spindle epochs (± 2.5 s), peak-locked. Given that we observed prominent power differences between young and older adults (Figure 1B), we normalized events per subjects by means of a z-score prior to all subsequent analyses, unless stated otherwise (Figure 2A). The mean and standard deviation were derived from the unfiltered event-locked average time course of either SO or spindle events (e.g. Figure 1C/D; lower right) in every participants. Z-scores were then computed for all trials and time points.

Event-locked spectral analysis: Time-frequency representations for artifact-free normalized SO (Figure 2B) were calculated after applying a 500 ms Hanning window. Spectral estimates (0.5 – 30 Hz; 0.5 Hz steps) were calculated between −2 and 2 s in steps of 50 ms and baseline-corrected by means of z-score relative to a bootstrapped baseline distribution that was created from all trials (baseline epoch −2 to −1.5s, 10000 iterations (Flinker et al., 2015)).

Event-locked cross-frequency coupling: For event-locked cross-frequency analyses (Dvorak and Fenton, 2014; Staresina et al., 2015), we first filtered the normalized SO trough-locked data (Figure 2D/E; spindle-locked in Figure 1C/D) into the SO component (0.1 – 1.25 Hz) and extracted the instantaneous phase angle after applying a Hilbert transform. Then we filtered the same trials between 12–16 Hz and extracted the instantaneous amplitude from the Hilbert transform. We only considered the time range from −2 to 2 s to avoid filter edge artifacts. For every subject, channel, and epoch, we now detected the maximal sleep spindle amplitude and corresponding SO phase angle. The mean circular direction and resultant vector length across all NREM events were determined using the CircStat toolbox. In addition, we divided the SO phase into 17 linearly spaced bins and calculated the mean sleep spindle amplitude per bin. We normalized the individual sleep spindle amplitude distribution by the mean across all bins.

Data-driven cross-frequency coupling: We calculated a comodulogram on 15-second artifact-free long non-overlapping z-normalized segments during NREM sleep. We calculated the modulation index (Canolty et al., 2006) between lower (0.5 – 6.5 Hz; 0.5 Hz steps) and faster frequencies (8–40 Hz; 1 Hz steps). For the low frequency, we utilized a

window of ± 1 Hz, which was adjusted for the lowest frequencies. For faster frequencies, the window was adjusted to capture the side peaks. Hence, the window at a given frequency was always defined as the low center frequency + 1Hz. I.e. at 15 Hz, the window to assess coupling to the 3 Hz phase was ± 4 Hz; while at 5 Hz the window was ± 6 Hz. The modulation index was normalized by a bootstrapped z-score relative to a distribution that was obtained by random-point block-swapping (200 iterations).

Cross-frequency directionality analysis: To determine whether low frequencies components drive sleep spindle activity during SWS or vice versa, we calculated the cross-frequency phase slope index (Jiang et al., 2015; Helfrich et al., 2017) between the normalized signal and the signal filtered in the sleep spindle range (12–16 Hz). To avoid edge artifacts, we restricted this analysis to ± 2seconds around the SO trough. Hence, these 4 second long segments include at least 3 cycles of the SO oscillation (~0.75 Hz), in accordance with previous reports (Jiang et al., 2015). We considered frequencies between 0.5 and 4 Hz (0.5 Hz steps; 0.25 Hz bandwidth) after applying a Hanning window and extracting the complex Fourier coefficients. Significant values above zero indicate that SO drive sleep spindle activity, while negative values indicate that sleep spindles drive SO. Values around zero indicate no directional coupling. We repeated this analysis based on 15 second long segments, which were then averaged across all available NREM events to demonstrate that the findings are not confounded by the chosen window length (Figure S2D).

Detection of SO and spindle frequency peaks

1. SO peak frequency (related to Figure 1B): In order to disentangle the true oscillatory SO component from the prominent 1/f slope, we utilized irregular-resampling auto-spectral analysis (IRASA; Wen and Liu, 2016). We analyzed non-overlapping 15 s segments of continuous artifact-free data during NREM sleep and assessed frequencies between 0.1 and 30 Hz. IRASA takes advantage of the fact that irregularly resampling of the neuronal signals by pairwise non-integer values (resampling factor rf and corresponding factor rf*: e.g. 1.1 and 0.9) slightly shifts the peak frequency of oscillatory signals by compressing or stretching the underlying signal. However, the 1/f component remains stable. This procedure is then repeated in small, overlapping windows (window size: 5 s, sliding steps: 1 s; resampling factors rf: 1.1–1.9 in 0.05 increments). Note resampling was always done in a pairwise fashion for factor h and the corresponding resampling factor rf* = 2 – rf. For each segment, we calculated the auto-power spectrum by means of a FFT after applying a Hanning window. Then all auto-spectra were median-averaged to obtain the power spectrum of the 1/f component, with the idea being that resampled oscillatory components are averaged out. Finally, the resampled 1/f PSD is subtracted from the original PSD to obtain the oscillatory residuals on which we performed the individual peak detection (SO range: peak < 2 Hz; spindle-range: 9–17 Hz).

2. In addition to IRASA, which provides a mean sleep spindle peak frequency, we also utilized a linear de-trending approach to assess spindle frequencies as a

function of the SO phase (Figure 3C), where we investigated whether SO modulates additional sleep spindle features besides the amplitude on a fine-grained temporal scale. Therefore, we screened every artifact-free normalized SO event (−1.25 to 1.25 around trough) at every channel separately for oscillatory activity in the sleep spindle range. First, we zero-padded every trial to 10 seconds to increase the frequency resolution (0.1 Hz), then applied a Hanning window and obtained spectral estimates between 8 and 16 Hz. The resulting power values were log transformed. The sleep spindle peak for every SO was detected after subtraction of linear fit to the spectrum to remove the 1/f component. Second, every trial was filtered at the trial-specific peak frequency (± 2 Hz) and the instantaneous amplitude was extracted from a Hilbert transform before we performed event-related cross-frequency coupling analyses. In addition, we only considered SO that contained sleep spindle events that exceeded the 75% percentile of sleep spindle amplitudes to ensure comparability for correlation analyses. This approach effectively corrected for differences in sleep spindle peak frequencies and spectral power distributions prior to correlation with behavior. To obtain time-resolved sleep spindle peak frequency estimates, we detected the sleep spindle peak as described above in a 500 ms sliding window approach. We shifted the window in 25ms steps relative to the SO events (−1 to 1s; ± 250 ms) and recalculated the sleep spindle peak frequency. Finally, we smoothed the resulting traces with 100ms moving average.

Structural MRI data analysis—To measure grey matter volume, optimized voxel-based morphometry (VBM) was performed using SPM8 (Penny et al., 2011) (Wellcome Department of Imaging Neuroscience) with the VBM8 toolbox (http://dbm.neuro.uni-jena.de/vbm.html) and the Diffeomorphic Anatomical Registration through Exponentiated Lie algebra (DARTEL) toolbox in order to improve registration of older brains to the normalized MNI template (Mak et al., 2011; Mander et al., 2013). To enhance signal to noise ratio, two T1-weighted MPRAGE images were first co-registered and averaged. Averaged images were then segmented applying the Markov random field approach (Rajapakse et al., 1997) and then registered, normalized, and modulated using DARTEL. Grey matter and white matter segmentations were inputted into DARTEL and utilized to create a study specific template, which was then used to normalize individual brains into MNI space. Modulated grey matter maps were then smoothed using an 8 mm Gaussian kernel.

Measures of total intracranial volume (TIV) for each participant were estimated from the sum of grey matter, white matter, and CSF segmentation, and then used to adjust grey matter volumetric measures to account for differences in head size. Given that slow oscillations, sleep spindles, and ripples depend on the interaction between prefrontal cortex, thalamus, and hippocampus regions, the Anatomical Automatic Labeling repository (Tzourio-Mazoyer et al., 2002) within the Wake Forest University PickAtlas toolbox (Maldjian et al., 2003) was used to generate anatomically-based ROIs for the hippocampus, thalamus, medial prefrontal cortex, and orbitofrontal cortex, as well as an occipital lobe control ROI. Mean voxelwise gray matter volume within anatomically defined ROIs were extracted using the Marsbar

toolbox (Brett et al., 2002) and used in analyses relating grey matter volumetric measures with sleep and memory variables.

Statistical analysis—Unless stated otherwise, we used cluster-based permutation tests (Maris and Oostenveld, 2007) to correct for multiple comparisons as implemented in FieldTrip (Monte Carlo method; 1000 iterations; maxsize criterion). Clusters were formed in time/frequency (e.g. Figure 2B/F) or space (e.g. Figure 2E/G) by thresholding independent t-tests (e.g. Figure 2E–G), circular-linear (e.g. Figure 3A/D) or linear correlations (Spearman, e.g. Figure 4A) at $p < 0.05$. Correlation values were transformed into t-values. A permutation distribution was then created by randomly shuffling labels. The permutation p-value was obtained by comparing the cluster statistic to the random permutation distribution. The clusters were considered significant at $p < 0.05$ (two-sided). Bonferroni-correction was applied to correct for multiple cluster tests (e.g. Figure 4B).

Circular statistics were calculated using the CircStat toolbox. Circular non-uniformity was assessed with Rayleigh tests at $p < 0.01$. Effect sizes were quantified by means of Cohen's d, the correlation coefficient rho or η^2 in case of repeated measures ANOVAs or Watson-Williams-tests (circular ANOVA equivalent). Circular-linear correlations were calculated according to the following formula:

$$\rho = \sqrt{\frac{r_{xs}^2 + r_{xc}^2 - 2 * r_{xs} * r_{xc} * r_{cs}}{1 - r_{cs}^2}}$$

where r_{xs}, r_{xc} and r_{cs} were defined as

$$r_{xs} = corr\,(x, sin\,(alpha))$$

$$r_{xc} = corr\,(x, cos\,(alpha))$$

$$r_{cs} = corr\,(sin\,(alpha)\,, cos\,(alpha))$$

with x being the linear and alpha being the circular variable. In order to control for confounding variables, we utilized partial correlations, where c was partialled out of x, sin(alpha) and cos(alpha) before computing the multiple correlation using the regression residuals. We utilized a threshold of 10% to define clusters following partial correlations, which were then again tested at a cluster alpha of 0.05 (Maris and Oostenveld, 2007). To obtain effect sizes for cluster tests, we calculated the effect size separately for all channel, frequency and/or time points and averaged across all data points in the cluster. Repeated-measures ANOVAs were Greenhouse-Geisser corrected.

DATA AND SOFTWARE AVAILABILITY

Freely available software and algorithms used for analysis are listed in the resource table. All custom scripts and data contained in this manuscript are available upon request from the Lead Contact.

KEY RESOURCE TABLE

REAGENT or RESOURCE	SOURCE	IDENTIFIER
Software and Algorithms		
MATLAB 2015a	MathWorks Inc.	RRID: SCR_001622
EEGLAB 13_4_4b	(Delorme and Makeig, 2004)	https://sccn.ucsd.edu/eeglab/index.php
FieldTrip 20161016	(Oostenveld et al., 2011)	http://www.fieldtriptoolbox.org/
CircStat 2012	(Berens, 2009)	https://philippberens.wordpress.com/code/circstats/
IRASA	(Wen and Liu, 2016)	https://purr.purdue.edu/publications/1987/1
SPM8	(Penny et al., 2011)	http://www.fil.ion.ucl.ac.uk/spm/
VBM8	(Ashburner and Friston, 2000)	http://dbm.neuro.uni-jena.de/vbm.html
DARTEL	(Mak et al., 2011)	Included in SPM
Anatomical Automatic Labeling	(Tzourio-Mazoyer et al., 2002)	included in SPM
Wake Forest University PickAtlas	(Maldjian et al., 2003)	http://fmri.wfubmc.edu/software/pickatlas
Marsbar	(Brett et al., 2002)	http://marsbar.sourceforge.net/

Supplementary Material

Refer to Web version on PubMed Central for supplementary material.

Acknowledgments

This work was supported by the Alexander von Humboldt Foundation (Feodor Lynen Program; RFH), R37NS21135 (RTK), R01AG034570 (WJJ), R01AG031164 (MPW), R01AG054019 (MPW), RF1AG054019 (MPW), R01MH093537 (MPW) and F32–AG039170 (BAM), all from the National Institutes of Health. We thank Joe Winer, David Baquirin, Maggie Belshe, Meghna Bhatter, Michelle Binod, Sam Bowditch, Catherine Dang, Jay Gupta, Amynta Hayenga, Danny Holzman, April Horn, Emily Hur, Jonathan Jeng, Samika Kumar, Candace Markeley, Elizabeth Mormino, Molly Nicholas, Sina Rashidi, Matthew Shonman, Lily Zhang, and Alyssa Zhu for their assistance, and Anthony Mander for his aid in task design.

References

Aru J, Aru J, Priesemann V, Wibral M, Lana L, Pipa G, Singer W, Vicente R. Untangling cross-frequency coupling in neuroscience. Curr Opin Neurobiol. 2015; 31:51–61. [PubMed: 25212583]

Ashburner J, Friston KJ. Voxel-based morphometry–the methods. NeuroImage. 2000; 11:805–821. [PubMed: 10860804]

Batterink LJ, Creery JD, Paller KA. Phase of Spontaneous Slow Oscillations during Sleep Influences Memory-Related Processing of Auditory Cues. J Neurosci Off J Soc Neurosci. 2016; 36:1401–1409.

Berens P. CircStat: A MATLAB Toolbox for Circular Statistics. J Stat Softw. 2009; 31:21.

Born J, Wilhelm I. System consolidation of memory during sleep. Psychol Res. 2012; 76:192–203. [PubMed: 21541757]

Brett M, Anton JL, Valabregue R, Poline JB. Region of interest analysis using the MarsBar toolbox for SPM 99. Neuroimage. 2002; 16:S497.

Buzsáki G. Memory consolidation during sleep: a neurophysiological perspective. J Sleep Res. 1998; 7(Suppl 1):17–23. [PubMed: 9682189]

Buzsáki G, Draguhn A. Neuronal oscillations in cortical networks. Science. 2004; 304:1926–1929. [PubMed: 15218136]

Canolty RT, Edwards E, Dalal SS, Soltani M, Nagarajan SS, Kirsch HE, Berger MS, Barbaro NM, Knight RT. High gamma power is phase-locked to theta oscillations in human neocortex. Science. 2006; 313:1626–1628. [PubMed: 16973878]

Clemens Z, Mölle M, Eross L, Barsi P, Halász P, Born J. Temporal coupling of parahippocampal ripples, sleep spindles and slow oscillations in humans. Brain J Neurol. 2007; 130:2868–2878.

Cole SR, Voytek B. Brain Oscillations and the Importance of Waveform Shape. Trends Cogn Sci. 2017; 21:137–149. [PubMed: 28063662]

De Gennaro L, Ferrara M. Sleep spindles: an overview. Sleep Med Rev. 2003; 7:423–440. [PubMed: 14573378]

Delorme A, Makeig S. EEGLAB: an open source toolbox for analysis of single-trial EEG dynamics including independent component analysis. J Neurosci Methods. 2004; 134:9–21. [PubMed: 15102499]

Diekelmann S, Born J. The memory function of sleep. Nat Rev Neurosci. 2010; 11:114–126. [PubMed: 20046194]

Dvorak D, Fenton AA. Toward a proper estimation of phase-amplitude coupling in neural oscillations. J Neurosci Methods. 2014; 225:42–56. [PubMed: 24447842]

Flinker A, Korzeniewska A, Shestyuk AY, Franaszczuk PJ, Dronkers NF, Knight RT, Crone NE. Redefining the role of Broca's area in speech. Proc Natl Acad Sci U S A. 2015; 112:2871–2875. [PubMed: 25730850]

Frankland PW, Bontempi B. The organization of recent and remote memories. Nat Rev Neurosci. 2005; 6:119–130. [PubMed: 15685217]

Gais S, Mölle M, Helms K, Born J. Learning-dependent increases in sleep spindle density. J Neurosci Off J Soc Neurosci. 2002; 22:6830–6834.

Gerber EM, Sadeh B, Ward A, Knight RT, Deouell LY. Non-Sinusoidal Activity Can Produce Cross-Frequency Coupling in Cortical Signals in the Absence of Functional Interaction between Neural Sources. PloS One. 2016; 11:e0167351. [PubMed: 27941990]

Helfrich RF, Knight RT. Oscillatory Dynamics of Prefrontal Cognitive Control. Trends Cogn Sci. 2016; 20:916–930. [PubMed: 27743685]

Helfrich RF, Schneider TR, Rach S, Trautmann-Lengsfeld SA, Engel AK, Herrmann CS. Entrainment of brain oscillations by transcranial alternating current stimulation. Curr Biol CB. 2014; 24:333–339. [PubMed: 24461998]

Helfrich RF, Huang M, Wilson G, Knight RT. Prefrontal cortex modulates posterior alpha oscillations during top-down guided visual perception. PNAS 1705965114v1-201705965. 2017

Isomura Y, Sirota A, Ozen S, Montgomery S, Mizuseki K, Henze DA, Buzsáki G. Integration and segregation of activity in entorhinal-hippocampal subregions by neocortical slow oscillations. Neuron. 2006; 52:871–882. [PubMed: 17145507]

Jiang H, Bahramisharif A, van Gerven MAJ, Jensen O. Measuring directionality between neuronal oscillations of different frequencies. NeuroImage. 2015; 118:359–367. [PubMed: 26025291]

Kitamura T, Ogawa SK, Roy DS, Okuyama T, Morrissey MD, Smith LM, Redondo RL, Tonegawa S. Engrams and circuits crucial for systems consolidation of a memory. Science. 2017; 356:73–78. [PubMed: 28386011]

Ladenbauer J, Ladenbauer J, Külzow N, de Boor R, Avramova E, Grittner U, Flöel A. Promoting sleep oscillations and their functional coupling by transcranial stimulation enhances memory consolidation in mild cognitive impairment. J Neurosci Off J Soc Neurosci. 2017

Latchoumane CFV, Ngo HVV, Born J, Shin HS. Thalamic Spindles Promote Memory Formation during Sleep through Triple Phase-Locking of Cortical, Thalamic, and Hippocampal Rhythms. Neuron. 2017

Lustenberger C, Boyle MR, Alagapan S, Mellin JM, Vaughn BV, Fröhlich F. Feedback-Controlled Transcranial Alternating Current Stimulation Reveals a Functional Role of Sleep Spindles in Motor Memory Consolidation. Curr Biol CB. 2016; 26:2127–2136. [PubMed: 27476602]

Mak HKF, Zhang Z, Yau KKW, Zhang L, Chan Q, Chu LW. Efficacy of voxel-based morphometry with DARTEL and standard registration as imaging biomarkers in Alzheimer's disease patients and cognitively normal older adults at 3.0 Tesla MR imaging. J Alzheimers Dis. 2011; 23:655–664. [PubMed: 21157022]

Mak-McCully RA, Rolland M, Sargsyan A, Gonzalez C, Magnin M, Chauvel P, Rey M, Bastuji H, Halgren E. Coordination of cortical and thalamic activity during non-REM sleep in humans. Nat Commun. 2017; 8:15499. [PubMed: 28541306]

Maldjian JA, Laurienti PJ, Kraft RA, Burdette JH. An automated method for neuroanatomic and cytoarchitectonic atlas-based interrogation of fMRI data sets. NeuroImage. 2003; 19:1233–1239. [PubMed: 12880848]

Mander BA, Rao V, Lu B, Saletin JM, Lindquist JR, Ancoli-Israel S, Jagust W, Walker MP. Prefrontal atrophy, disrupted NREM slow waves and impaired hippocampal-dependent memory in aging. Nat Neurosci. 2013; 16:357–364. [PubMed: 23354332]

Mander BA, Rao V, Lu B, Saletin JM, Ancoli-Israel S, Jagust WJ, Walker MP. Impaired prefrontal sleep spindle regulation of hippocampal-dependent learning in older adults. Cereb Cortex N Y N 1991. 2014; 24:3301–3309.

Mander BA, Marks SM, Vogel JW, Rao V, Lu B, Saletin JM, Ancoli-Israel S, Jagust WJ, Walker MP. β-amyloid disrupts human NREM slow waves and related hippocampus-dependent memory consolidation. Nat Neurosci. 2015; 18:1051–1057. [PubMed: 26030850]

Mander BA, Winer JR, Walker MP. Sleep and Human Aging. Neuron. 2017; 94:19–36. [PubMed: 28384471]

Maris E, Oostenveld R. Nonparametric statistical testing of EEG- and MEG-data. J Neurosci Methods. 2007; 164:177–190. [PubMed: 17517438]

Marshall L, Helgadóttir H, Mölle M, Born J. Boosting slow oscillations during sleep potentiates memory. Nature. 2006; 444:610–613. [PubMed: 17086200]

Mitra PP, Pesaran B. Analysis of dynamic brain imaging data. Biophys J. 1999; 76:691–708. [PubMed: 9929474]

Mölle M, Marshall L, Gais S, Born J. Grouping of spindle activity during slow oscillations in human non-rapid eye movement sleep. J Neurosci Off J Soc Neurosci. 2002; 22:10941–10947.

Mölle M, Bergmann TO, Marshall L, Born J. Fast and slow spindles during the sleep slow oscillation: disparate coalescence and engagement in memory processing. Sleep. 2011; 34:1411–1421. [PubMed: 21966073]

Murphy M, Riedner BA, Huber R, Massimini M, Ferrarelli F, Tononi G. Source modeling sleep slow waves. Proc Natl Acad Sci U S A. 2009; 106:1608–1613. [PubMed: 19164756]

Niknazar M, Krishnan GP, Bazhenov M, Mednick SC. Coupling of Thalamocortical Sleep Oscillations Are Important for Memory Consolidation in Humans. PloS One. 2015; 10:e0144720. [PubMed: 26671283]

Nir Y, Staba RJ, Andrillon T, Vyazovskiy VV, Cirelli C, Fried I, Tononi G. Regional slow waves and spindles in human sleep. Neuron. 2011; 70:153–169. [PubMed: 21482364]

Oostenveld R, Fries P, Maris E, Schoffelen JM. FieldTrip: Open source software for advanced analysis of MEG, EEG, and invasive electrophysiological data. Comput Intell Neurosci. 2011; 2011:156869. [PubMed: 21253357]

Papalambros NA, Santostasi G, Malkani RG, Braun R, Weintraub S, Paller KA, Zee PC. Acoustic Enhancement of Sleep Slow Oscillations and Concomitant Memory Improvement in Older Adults. Front Hum Neurosci. 2017; 11:109. [PubMed: 28337134]

Penny, WD., Friston, KJ., Ashburner, JT., Kiebel, SJ., Nichols, TE. Statistical parametric mapping: the analysis of functional brain images. Academic press; 2011.

Prerau MJ, Brown RE, Bianchi MT, Ellenbogen JM, Purdon PL. Sleep Neurophysiological Dynamics Through the Lens of Multitaper Spectral Analysis. Physiol Bethesda Md. 2017; 32:60–92.

Rajapakse JC, Giedd JN, Rapoport JL. Statistical approach to segmentation of single-channel cerebral MR images. IEEE Trans Med Imaging. 1997; 16:176–186. [PubMed: 9101327]

Rasch B, Born J. About sleep's role in memory. Physiol Rev. 2013; 93:681–766. [PubMed: 23589831]

Rechtschaffen A, Kales A. A manual of standardized terminology, techniques, and scoring systems for sleep stages of human subjects. 1968

Riedner BA, Hulse BK, Murphy MJ, Ferrarelli F, Tononi G. Temporal dynamics of cortical sources underlying spontaneous and peripherally evoked slow waves. Prog Brain Res. 2011; 193:201–218. [PubMed: 21854964]

Rosanova M, Ulrich D. Pattern-specific associative long-term potentiation induced by a sleep spindle-related spike train. J Neurosci Off J Soc Neurosci. 2005; 25:9398–9405.

Saletin JM, van der Helm E, Walker MP. Structural brain correlates of human sleep oscillations. NeuroImage. 2013; 83:658–668. [PubMed: 23770411]

Sirota A, Csicsvari J, Buhl D, Buzsáki G. Communication between neocortex and hippocampus during sleep in rodents. Proc Natl Acad Sci U S A. 2003; 100:2065–2069. [PubMed: 12576550]

Staresina BP, Bergmann TO, Bonnefond M, van der Meij R, Jensen O, Deuker L, Elger CE, Axmacher N, Fell J. Hierarchical nesting of slow oscillations, spindles and ripples in the human hippocampus during sleep. Nat Neurosci. 2015; 18:1679–1686. [PubMed: 26389842]

Steriade M. Grouping of brain rhythms in corticothalamic systems. Neuroscience. 2006; 137:1087–1106. [PubMed: 16343791]

Steriade M, Domich L, Oakson G, Deschênes M. The deafferented reticular thalamic nucleus generates spindle rhythmicity. J Neurophysiol. 1987; 57:260–273. [PubMed: 3559675]

Tzourio-Mazoyer N, Landeau B, Papathanassiou D, Crivello F, Etard O, Delcroix N, Mazoyer B, Joliot M. Automated anatomical labeling of activations in SPM using a macroscopic anatomical parcellation of the MNI MRI single-subject brain. NeuroImage. 2002; 15:273–289. [PubMed: 11771995]

Walker MP, Stickgold R. Sleep, memory, and plasticity. Annu Rev Psychol. 2006; 57:139–166. [PubMed: 16318592]

Wen H, Liu Z. Separating Fractal and Oscillatory Components in the Power Spectrum of Neurophysiological Signal. Brain Topogr. 2016; 29:13–26. [PubMed: 26318848]

Highlights

- Precise coupling of NREM slow waves and spindles dictates memory consolidation.
- Aging impairs slow wave-spindle coupling, leading to overnight forgetting.
- Age-related atrophy in mPFC predicts the failure of such coupling and thus memory.

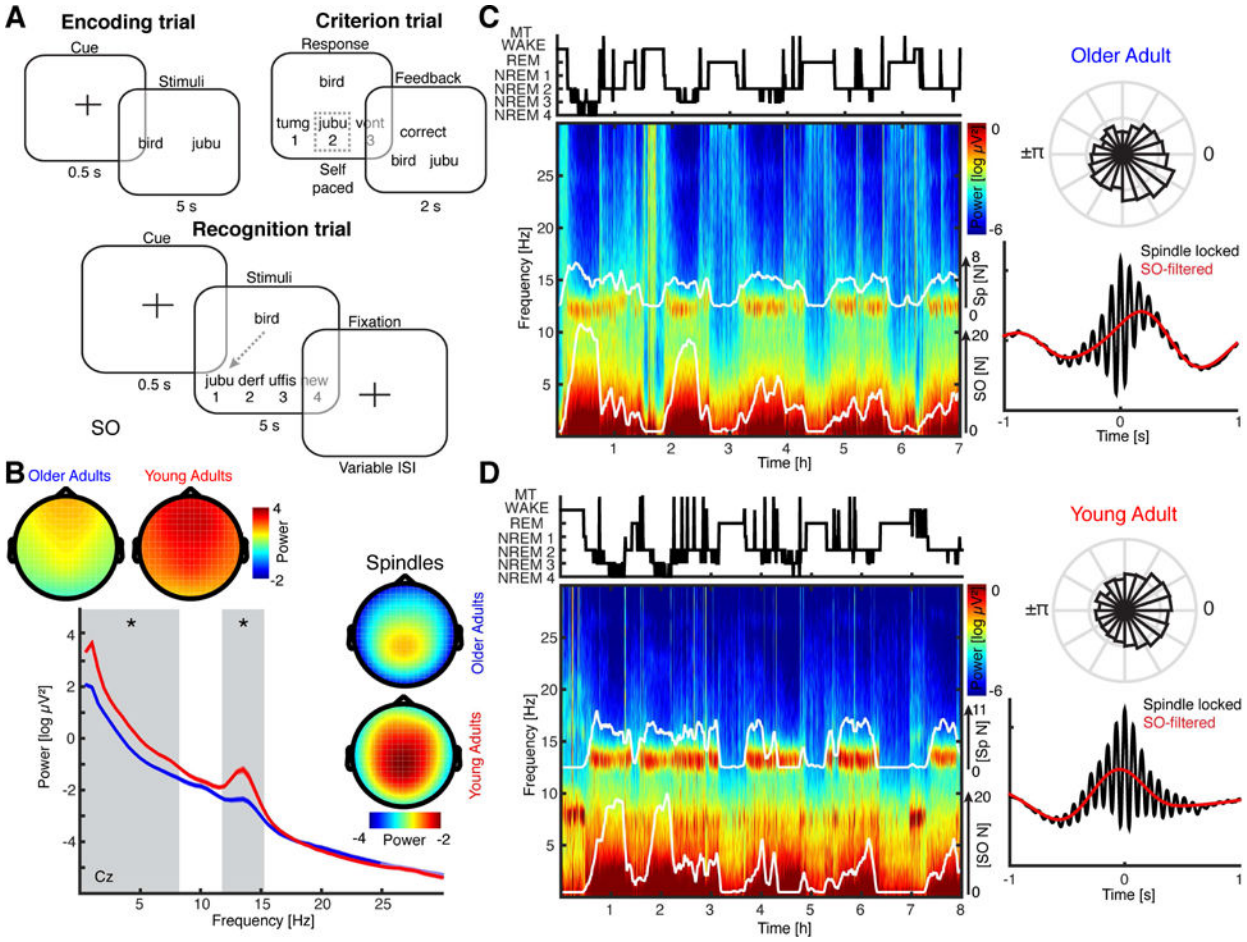

Figure 1. Memory task and oscillatory signatures of sleep

(a) Episodic word-pair task. Participants learned 120 word-nonsense word pairs. Nonsense words were 6–14 letters in length, derived from groups of common phonemes. During encoding trials (upper left) word pairs were presented for 5s. Participants completed the criterion training (upper right) directly after encoding and received feedback after every trial. Recognition trials (lower panel) were performed after a short delay (10min, 45 trials) and again after a full night of sleep (10h, 135 trials). (b) EEG power spectra during NREM sleep at electrode Cz for older (blue) and young (red) adults (mean ± SEM). Grey shaded areas indicate significant differences in low and sleep spindle frequency ranges. Insets depict topographical distribution of SO (<1.5 Hz; upper topographies) and sleep spindle (12–16 Hz; topographies on the right) power. Note that older subjects exhibited significantly reduced oscillatory power across the whole head. (c) Upper left: Hypnogram (MT = movement time) from one exemplary of older subject and full night multi-taper spectrogram at Pz (lower left) with superimposed number of detected SO and sleep spindle events (white solid lines; 5min averages). Upper right: Normalized circular histogram of detected spindle events relative to the SO phase. Note the peak in the right lower quadrant. Lower right: Peak-locked sleep spindle average across all detected events in NREM sleep (black). Low-pass filtered events (red) highlight that the sleep spindles preferentially peaked prior to the

SO ‘up-state’. See also Figure S1A. (d) Exemplary young subject. Same conventions as in panel c. Note, the sleep spindle amplitude is maximal after the SO peak.

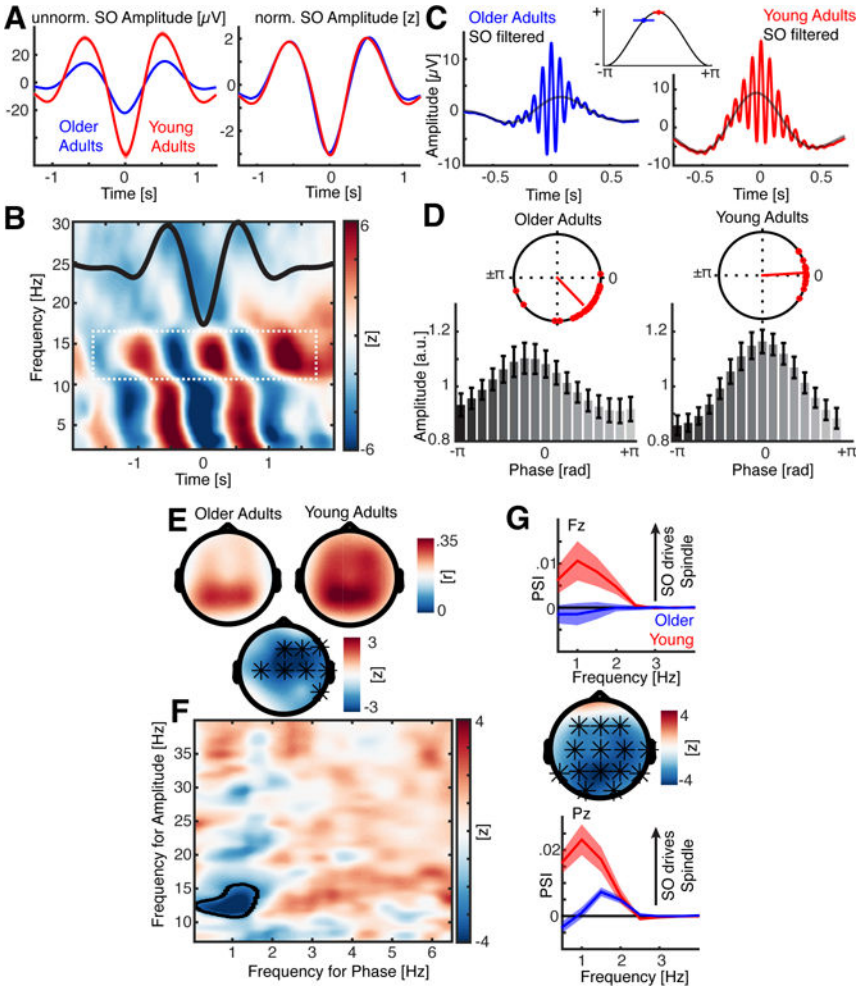

Figure 2. SO-Spindle interactions in old and young adults

(a) Left: Trough-locked SO grand average for old (blue) and young (red) adults. Note the prominent differences in amplitude. Right: We normalized the SO amplitude for every subject prior to all other analyses to alleviate spurious effects, which could be the result of prominent power and signal-to-noise differences (mean ± SEM). (b) Statistical map of SO-locked power differences across time between older and young subjects. Note the interleaved patterning in the sleep spindle range (12–16 Hz; white dashed box). As reference, the mean SO is superimposed (black; rescaled). See also Figure S2A. (c) Left: Peak-locked spindle grand-averages for old adults with superimposed low-pass filtered signal (black). Red: Peak-locked sleep spindle grand-average for young adults. Top: Averaging mean coupling phase and SD on schematic SO (cosine). (d) Upper: Mean SO phase where sleep spindle power peaks. Red dots depict individual subjects. Note sleep spindle power in older adults peaks prior to the SO positive peak (0°), while sleep spindle power in young subjects peaks around 0°. Lower: Grand-average normalized spindle amplitu de binned relative to the SO phase (mean ± SEM). Again, note the non-uniform distribution, which peaks around 0° for young adults, but earlier for older a dults. See also Figure S1D–H. (e) Upper: SO-spindle coupling strength (resultant vector length) topography for old (left) and young (right) adults. Lower: A statistical difference map (center) indicates that the

coupling strength was significantly reduced for fronto-central EEG sensors, while parieto-occipital estimates did not differ (* denotes cluster-corrected two-sided $p < 0.05$). (f) Statistical map of a data-driven comodulogram. The black-circled area highlights the significant difference between older and young adults, which was confined to the SO-spindle range. See also Figure S2B. (g) Cross-frequency directionality analyses. Values above zero indicate that SO drive sleep spindle activity. Upper: We found that frontal SO drive sleep spindle activity in young but not older adults (electrode Fz; mean ± SEM), while parieto-occipital SO predicts sleep spindle activity in both older and young adults (lower panel; Pz; Figure S2C). However, this effect is pronounced for young adults. The topography (center panel) depicts the spatial extent where directional SO-spindle influences are reduced in older relative to young adults. Note that this effect was independent of the chosen window length (Figure S2D).

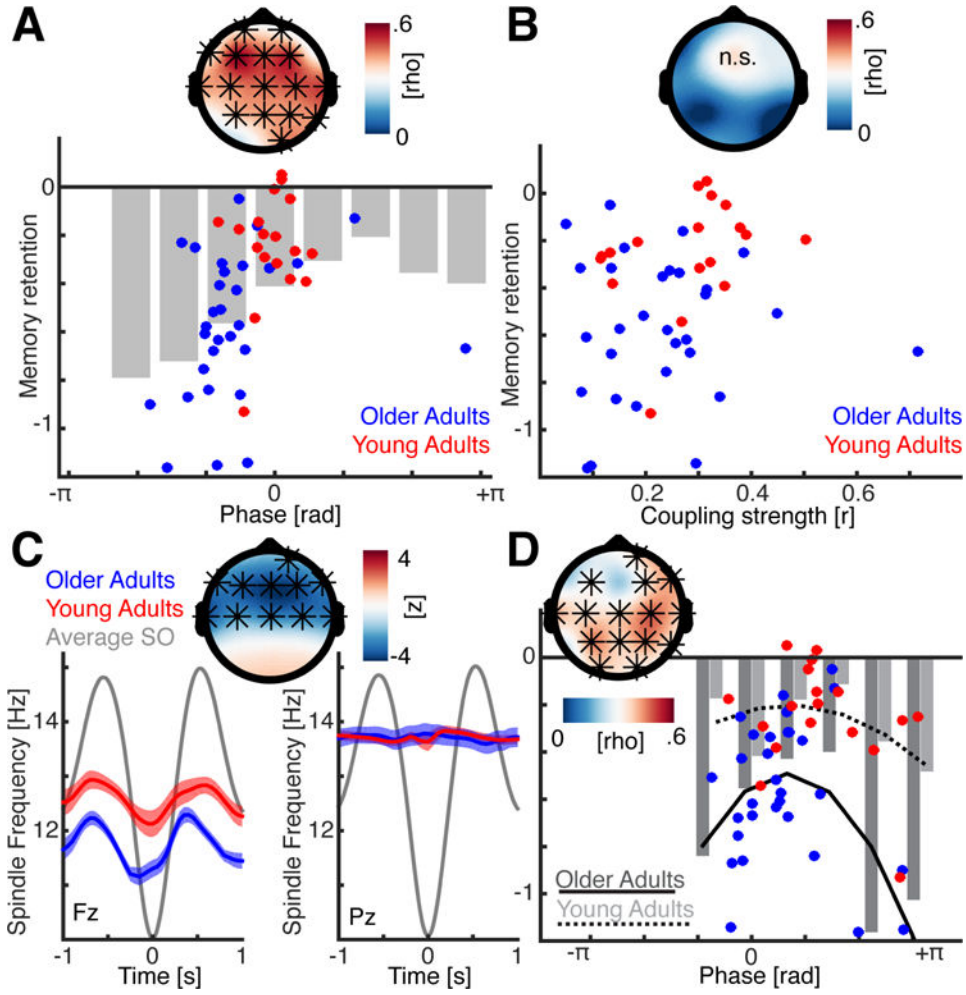

Figure 3. Timing of SO-spindle interactions predicts memory retention

(a) Upper: Cluster-corrected circular-linear correlation analysis between the individual mean SO-spindle coupling phase and overnight memory retention after correction for power differences (* indicates significant sensors). The strongest effect was observed at electrode F3. Lower: Blue dots indicate older adults; red dots young adults. We binned the mean behavioral performance relative to the coupling phase in 10 overlapping bins to highlight the u-shaped, non-linear relationship. (b) No significant correlation was observed between coupling strength (resultant vector length) and memory retention (same conventions as in panel A). (c) Sleep spindle frequency relative to SO cycle at a frontal (left) and parieto-occipital (Pz; right) electrode (mean ± SEM). Frontal sleep spindles are slower than posterior sleep spindles. Their frequency only varies as a function of the SO phase over frontal regions where it is significantly lower for older adults (top panel). (d) Cluster-corrected circular-linear correlations after correcting for differences in power distributions and sleep spindle frequencies (see also Figure S3; same conventions as in panel A). Importantly, memory retention was coupling phase dependent in older and young adults. Overall the best performance was observed when the sleep spindles peak just after the SO peak. Blue dots depict older adults. Dark grey bars indicate mean binned memory performance; black solid line depicts a quadratic fit to approximate the non-linear u-shaped

relationship. Conversely, red dots, light grey bars and the dashed black line reflect young adults.

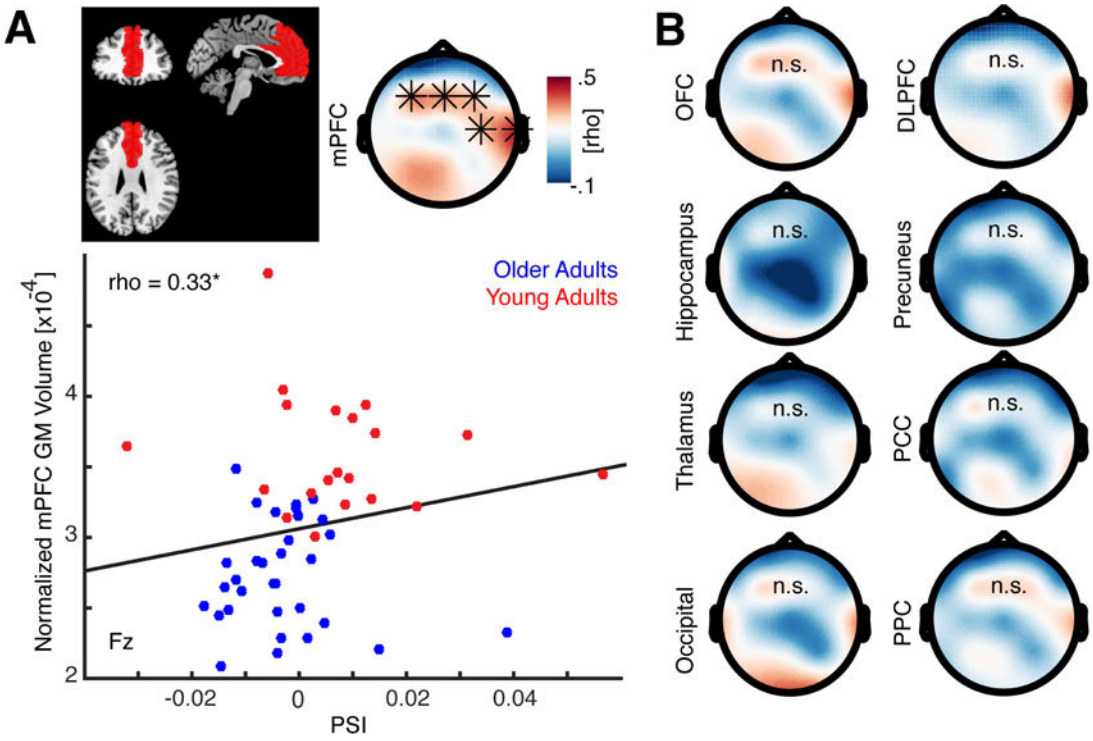

Figure 4. Directional SO-spindle coupling depends on prefrontal grey matter volume

(a) Upper right: Definition of the mPFC ROI on coronal, sagittal and axial slices. Upper left: Topographic map of cluster-corrected correlation analysis between grey matter (GM) volume and the directional CFC (PSI), which revealed that directional influences were stronger when subjects' had more GM volume. Lower panel: Scatter plot of significant correlation at electrode Fz. Hence, age-related GM atrophy contributes to a breakdown of SO-mediated spindle coupling. Note that GM volume was corrected for age-related total intracranial volume. (b) This significant relationship was limited to mPFC, and was not observed in other select regions including the hippocampus, thalamus, adjacent regions such as the OFC and DLPFC, nor in any of additional control regions (occipital, precuneus, posterior cingulate and posterior parietal).